

SCIENTIFIC REPORTS



OPEN

Change in the site density and surface acidity of clay minerals by acid or alkali spills and its effect on pH buffering capacity

Inhyeong Jeon & Kyoungphile Nam

Changes in the site density and surface acidity constants (i.e. pK_{a1} and pK_{a2}) of kaolinite and montmorillonite were determined after acid or alkali spills, and pH buffering capacity was evaluated as a parameter of soil function change. Surface complexation modeling with potentiometric titrations and Fourier-transform infrared spectroscopy showed that acid or alkali spills did not significantly change the surface properties of kaolinite. In montmorillonite, however, acid spills decreased the basal site density from 832 to 737 mmol kg^{-1} by dissolving substituted octahedral cations and decreased pK_{a2} from 7.32 to 5.42 by dissolving SiOH. In response to alkali spills, the basal site density increased to 925 mmol kg^{-1} , and the edge site density increased from 84.8 to 253 mmol kg^{-1} due to AlOH and SiOH formation; thus, pK_{a2} decreased to 6.78. The pH buffering capacity of acid- or alkali-spilled kaolinite at pH 6 did not significantly change, while that of acid- or alkali-spilled montmorillonite increased from 30.3 to 35.9 and 56.0 mmol kg^{-1} , respectively. Our results indicate that these spills greatly altered the surface properties of montmorillonite, but unexpectedly, increased the pH buffering capacity of montmorillonite.

As the chemical industry develops, chemical accidents occur annually, and of them, acid or alkali spills are of great concern because of their high frequency and hazard¹. According to the Chemistry Safety Clearing-house database², acid or alkali spills accounted for 46% of the chemical accidents in South Korea^{3,4}. If acid or alkali spills onto soil, most of the physicochemical properties of soil are altered, such as pH, organic matter content, base saturation, exchangeable cations, and surface area^{5–9}. Although neutralizers have been poured onto acid- or alkali-spilled soils for pH recovery^{10,11}, neutralization cannot recover nonreversible dissolution of organic matter or clay minerals and the change in cation exchange capacity (CEC) caused by the structural deterioration¹². Changes in these properties will alter soil functions, particularly pH buffering capacity. Because pH buffering capacity is related to soil productivity and the water quality of stream water near soil¹³, studies of the change in pH buffering capacity of acid- or alkali-spilled soil after neutralization are needed.

For this purpose, the effects of acid or alkali spills on organic matter and clay minerals, the soil constituents that determine the pH buffering capacity of soils, should be analyzed. In the case of organic matter, acid or alkali spills desorb or dissolve it^{14–16}; thus, the pH buffering capacity decreases. However, the effect of these spills on clay minerals is unclear. Little attention has been paid on changes in clay minerals' properties due to these spills. Only a few studies revealed that an acid or alkali treatment at room temperature over two weeks not only altered a crystal structure of clay minerals but also increased surface area⁸. Instead, many studies have focused on an acid or alkali activation treating clay minerals with high concentration of acid or alkali, and its effect on clay minerals' surface area, porosity and surface acidity^{17–19}. Also, there have been several studies on soil acidification phenomenon, and they revealed that the long-term acidification led to chemical weathering of clay minerals and decreased the base saturation^{20–22}.

However, these reaction conditions are unrealistic in natural environment after acid or alkali spills. To predict the pH buffering capacity of acid- or alkali-spilled clay minerals, clay minerals' site density and surface reaction constants should be determined. It has been known that two major pH buffering reactions of clay minerals are protonation or deprotonation reaction of edge sites, and proton exchange reaction of basal sites^{23,24}. Previous studies have successfully identified the site density of surface functional groups in clay minerals and their surface

Department of Civil and Environmental Engineering, Seoul National University, Seoul, 08826, Republic of Korea. Correspondence and requests for materials should be addressed to K.N. (email: kpnam@snu.ac.kr)

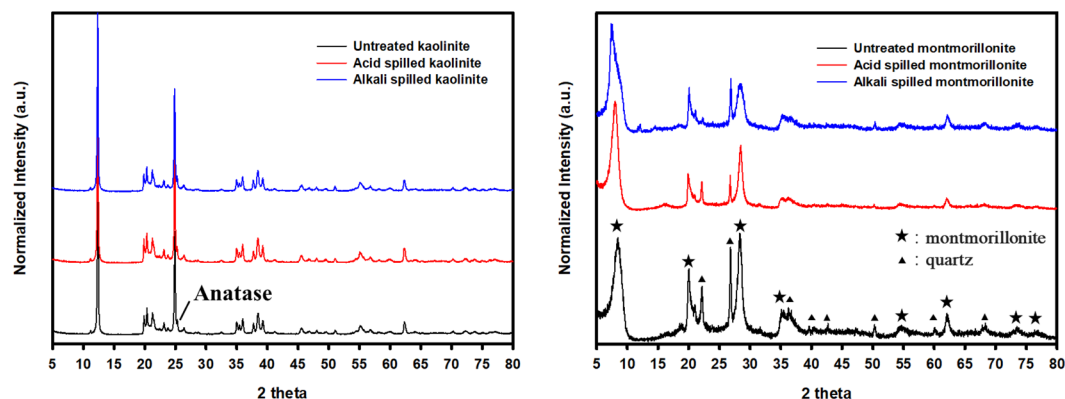


Figure 1. XRD patterns of three different (left) kaolinite and (right) montmorillonite samples. Black, red, and blue lines represent the XRD patterns of untreated, acid-spilled, and alkali-spilled clay minerals, respectively. Kaolinite and montmorillonite contained an anatase and a quartz as an impurity, respectively, which is consistent with the previous baseline study on the XRD patterns of KGa-1b kaolinite and Swy-2 montmorillonite²⁴.

Clay minerals	Condition	Concentration of Dissolved Constituent Elements			
		Al	Si	Fe	Mg
mg (g clay minerals) ⁻¹					
Kaolinite	Acid	2.67 ± 0.15	0.74 ± 0.04	0.25 ± 0.01	0.03 ± 0.00
	Alkali	21.8 ± 1.00	25.0 ± 2.3	0.48 ± 0.14	0.02 ± 0.00
Montmorillonite	Acid	9.09 ± 1.56	18.8 ± 6.2	11.3 ± 1.19	1.99 ± 0.34
	Alkali	1.24 ± 0.28	104 ± 11.5	2.61 ± 0.16	0.11 ± 0.06

Table 1. Dissolution of the clay minerals' constituent elements by acid or alkali spills measured by ICP-OES. The concentration of dissolved elements are the average values of triplicate experiments.

reaction constants using surface complexation modeling^{25,26}. Nevertheless, a few studies exist investigating alterations of surface properties of clay minerals at ambient temperature following intensive acid or alkali treatment, which is similar to acid or alkali spills, by using surface complexation modeling. In addition, clay minerals play a significant role in the pH buffering capacity of soils with low organic matter content resulting from acid or alkali spills; thus, knowledge of the changes in clay minerals' properties after these spills is essential to interpret the pH buffering capacity of the soils.

The goals of this study were to investigate changes in the site density and surface reaction constants of the neutralized clay minerals after acid or alkali spills and evaluate their effect on the pH buffering capacity as an indicator of soil function. Kaolinite (KGa-1b, Georgia) and montmorillonite (SWy-3, Wyoming), which are typical 1:1 and 2:1 clay minerals, respectively, were selected in this study. Three different samples (untreated, acid-spilled, and alkali-spilled) were prepared by treating with deionized water, 5 M HCl, and 5 M NaOH, respectively, and they were neutralized, and their surface properties before and after acid or alkali spills were compared. The site density and surface acidity constants were determined by a potentiometric titration using surface complexation modeling, and the change in the pH buffering capacity resulting from acid or alkali spills was investigated.

Results and Discussion

XRD characterization of three different clay minerals. The XRD patterns of three different kaolinite and montmorillonite samples are shown in Fig. 1, and the results of quantitative analysis are summarized in Supplementary Table S1. The untreated kaolinite and montmorillonite were mainly composed of pure kaolinite (98%) and montmorillonite (79%), respectively. The untreated kaolinite contained an anatase (2%), and the untreated montmorillonite contained a quartz (13%) and cristobalite (8%). The results are consistent with the previous baseline study on the XRD patterns of KGa-1b kaolinite and Swy-2 montmorillonite²⁷.

The XRD patterns and quantitative analysis showed that while acid or alkali spills had little effect on the crystalline structure and the mineral identity of kaolinite, they had some effects on those of montmorillonite. Newly formed constituents were not observed in both acid- or alkali-spilled kaolinite and montmorillonite. The proportions of kaolinite and anatase in both acid- and alkali-spilled kaolinite did not change as a result of each spill. In montmorillonite samples, however, acid spills did not significantly change the proportion of montmorillonite, while decreased that of quartz to 4% and increased that of cristobalite to 14%. Alkali spills increased the proportion of montmorillonite to 88%, while decreased those of quartz and cristobalite to 9 and 3%, respectively.

Dissolution of major elements of clay minerals by acid or alkali spills. The concentrations of dissolved elements of kaolinite and montmorillonite as a result of acid or alkali spills are summarized in the Table 1.

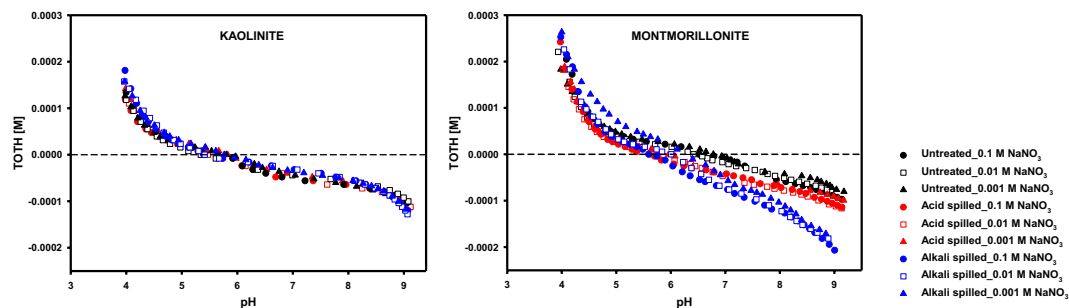


Figure 2. Titration curves of three different (left) kaolinite and (right) montmorillonite samples obtained from potentiometric titrations. The Y-axis is the molar concentration of the total added proton in the solution. The black, red, and blue symbols represent untreated, acid-spilled, and alkali-spilled kaolinite or montmorillonite, respectively, and the circle-, rectangle-, and triangle-shaped symbols represent a 0.1, 0.01, and 0.001 M NaNO_3 condition, respectively. All experimental data were well fitted with predicted titration curves using SCM (see Supplementary Fig. S1).

	Kaolinite			Montmorillonite		
	Untreated	Acid-spilled	Alkali-spilled	Untreated	Acid-spilled	Alkali-spilled
Surface reaction constants (pK)						
$\equiv \text{SOH}_2^+ \leftrightarrow \equiv \text{SOH} + \text{H}^+$ (pK_{a_1})	-4.55	-4.38	-4.72	-5.79	-5.93	-5.00
$\equiv \text{SOH}_2^+ \leftrightarrow \equiv \text{SOH}^- + \text{H}^+$ (pK_{a_2})	5.49	5.94	6.34	7.32	5.42	6.78
$\equiv \text{X}^- \cdot \text{Na}^+ + \text{H}^+ \leftrightarrow \equiv \text{X}^- \cdot \text{H}^+ + \text{Na}^+$ (pK_{H})	-2.90 ^a	-2.90 ^a	-2.90 ^a	1.51	0.72	1.85
Functional group density						
Edge site density (mmol kg^{-1})	35.8	40.6	38.6	84.8	85.3	253.2
Basal site density (mmol kg^{-1})	8.3	5.9	8.2	832.0	737.0	925.0

Table 2. Optimized surface properties of three different kaolinite and montmorillonite samples using FITEQL. The K_{a_1} , K_{a_2} , edge site density and basal site density were fitting parameters and optimized. In montmorillonite samples, K_{H} was also included in fitting parameters. The detailed procedure of parameter optimization is summarized in the Supplementary Information. ^aNot determined by optimization, but the average value of other research^{55,68–70}.

The dissolved Al and Si concentrations of kaolinite after acid spill were $2.67 \text{ mg-Al g}^{-1}$ and $0.737 \text{ mg-Si g}^{-1}$, respectively, and those after alkali spill were $21.8 \text{ mg-Al g}^{-1}$ and $25.0 \text{ mg-Si g}^{-1}$, respectively. Kaolinite was more susceptible to alkali spill than to acid spill. In the case of montmorillonite, while the dissolved Al and Si concentrations after acid spill were $9.09 \text{ mg-Al g}^{-1}$ and $18.8 \text{ mg-Si g}^{-1}$, respectively, those after alkali spill were $1.24 \text{ mg-Al g}^{-1}$ and 103 mg-Si g^{-1} , respectively. While more than five times of the octahedral cations such as Al, Fe and Mg were dissolved by acid spill than by alkali spill, the tetrahedral cation, Si, was dissolved five times more by alkali spill than by acid spill. The high dissolution of octahedral cations as a result of acid spill was probably because protons preferentially attack the isomorphically substituted elements in octahedral sheet during acid treatment²⁸.

Irreversible alteration on site density and surface acidity constants resulting from acid or alkali spills. The titration curves of three different kaolinite and montmorillonite samples under different NaNO_3 concentration are shown in Fig. 2. As shown, acid or alkali spills have a greater effect on the titration curves of montmorillonite than those of kaolinite, and the background electrolytic concentration had a limited effect on the titration curves of both kaolinite and montmorillonite at pH values of 4–9. The reversibility test of three different kaolinite and montmorillonite samples under 0.01 M NaNO_3 are shown in Supplementary Fig. S3. Although some hysteresis was observed, it was not pronounced. It could be because the factors such as CO_2 input and dissolutions of clay minerals were controlled during the experiments²⁹. The optimized values of the surface properties obtained from FITEQL 4.0 are summarized in Table 2.

Table 2 shows that an acid or alkali spill did not significantly change the edge and basal site density, which refers to variable charged sites on the mineral edges and permanent negatively charged sites on basal planes, respectively, of kaolinite (i.e. less than 5 mmol kg^{-1}). An acid or alkali spill increased the edge site density of kaolinite from 35.8 to 40.6 and $38.6 \text{ mmol kg}^{-1}$, respectively, and changed the basal site density of kaolinite from 8.3 to 5.9 and 8.2 mmol kg^{-1} , respectively. In the case of montmorillonite, an acid or alkali spill significantly changed the edge and basal site density (i.e. greater than 100 mmol kg^{-1}) except for the edge site density of the acid-spilled montmorillonite. An alkali spill greatly increased the edge site density from 84.8 to $253.2 \text{ mmol kg}^{-1}$. In addition, an acid or alkali spill changed the basal site density from 832 to 737 and 925 mmol kg^{-1} , respectively.

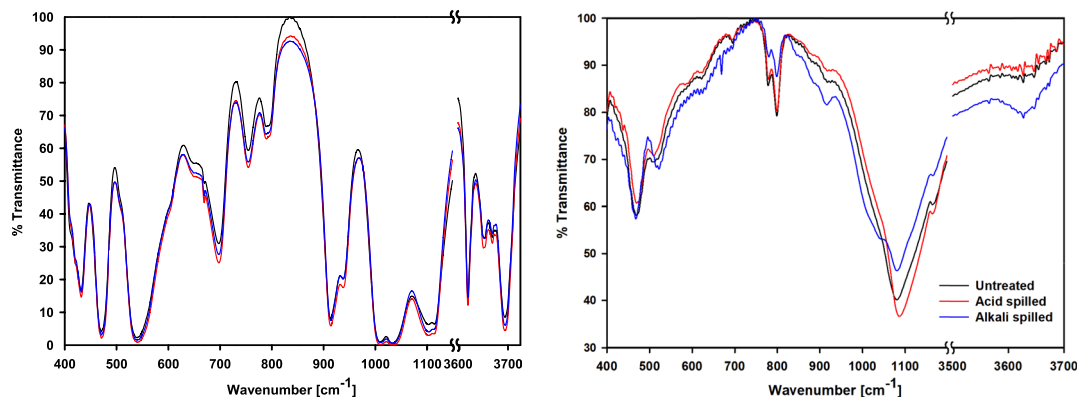


Figure 3. FT-IR spectra of (left) kaolinite and (right) montmorillonite. Black, red, and blue lines represent untreated, acid-spilled, and alkali-spilled kaolinite or montmorillonite.

Regarding the surface acidity constants (i.e. pK_{a1} and pK_{a2}), an acid or alkali spill did not cause meaningful changes in the kaolinite (i.e. less than a 0.5 pK_a value) except the pK_{a2} of the alkali-spilled kaolinite increased from 5.49 to 6.34. In the case of montmorillonite, the pK_a values greatly changed compared to those of the kaolinite (i.e. greater than a 0.5 pK_a value) except for the pK_{a1} value of the acid-spilled montmorillonite. The pK_{a1} value of the alkali-spilled montmorillonite increased from -5.79 to -5.00 , while the pK_{a2} value of the acid-spilled montmorillonite greatly decreased from 7.32 to 5.42 and that of the alkali-spilled montmorillonite decreased to 6.78. In addition, the proton exchange reaction constant of montmorillonite (pK_H) changed from 1.51 to 0.72 and 1.85 as a result of an acid or alkali spill, respectively.

According to the Fig. 2, titration curves of the kaolinite and montmorillonite only slightly changed under the different concentrations of background electrolyte. In the case of kaolinite, this was probably because the edge site density was approximately five times higher than the basal site density, which was consistent with previous studies^{24,30}. Thus, the effect of the proton exchange reaction of the kaolinite's basal sites on the titration curve was relatively small in a range of pH 4–9 (see Supplementary Fig. S2). In contrast to the kaolinite, the basal site density of montmorillonite was approximately 5–10 times higher than its edge site density, which was consistent with previous research summarized in Bourg *et al.*²⁵. However, the concentration of the electrolyte also had a slight effect on the titration curves of montmorillonite, and this might be because montmorillonite used in this study has a high affinity to Na^+ . Basal sites were saturated with Na^+ at pH values of 4–9; thus, the proton exchange reaction could be negligible within this pH range (see Supplementary Fig. S2). This indicated that the pH buffering of both kaolinite and montmorillonite was largely determined by the edge site reactions rather than those of the basal sites at pH 4–9. Thus, it is reasonable that the larger change in the titration curves of the montmorillonite compared to that of the kaolinite resulting from acid or alkali spills was probably because of the greater alterations on the edge sites' properties in the montmorillonite.

Structural modification due to acid or alkali spills. FT-IR spectra of the three different kaolinite and montmorillonite samples are shown in Fig. 3; the band assignments of the Clay Minerals Society's source clay (KGa-1b kaolinite, Swy-2 montmorillonite) were used in this study^{31,32}. All absorption bands, particularly the Si-O of the tetrahedral sheet at 400–1100 cm^{-1} , Si-O-Si at 472 cm^{-1} , Al-O-Si of the octahedral sheet at 541 cm^{-1} , and the OH hydroxyl groups at 915, 938, and 3600–3700 cm^{-1} , of the untreated kaolinite were observed and the positions of the bands were nearly the same as the reference. However, the untreated montmorillonite (Swy-3) used in this study had a similar but slightly different shape and position of bands compared to the Swy-2 montmorillonite in the reference. The absorption band assigned for Al-O-Si, found in Swy-2 at 524 cm^{-1} , was observed near 512 cm^{-1} , and the band assigned for the Si-O of the tetrahedral sheet, found in Swy-2 montmorillonite at 1041 cm^{-1} , was not observed in the untreated montmorillonite. Instead, the strong band at 1080 cm^{-1} was observed, and it might be because the untreated montmorillonite contained some quartz and cristobalite whose bands assigned to the Si-O were observed near 1080 cm^{-1} ³¹. It is supported by the FT-IR spectra observed at 778 and 798 cm^{-1} , which are assigned to the Si-O of quartz and cristobalite, respectively. These results are consistent with the result of XRD analysis (Fig. 1 and Table S1) and the FT-IR baseline study. The other bands were similar to those of the Swy-2 montmorillonite. Absorption bands at 842, 885, and 917 cm^{-1} were assigned to octahedral sites where isomorphic substitution occurred, and the band at 3627 cm^{-1} was assigned to the hydroxyl groups of octahedral cations, particularly Al^{3+} ³³.

Acid or alkali spills did not significantly change the FT-IR spectra of the kaolinite. All the absorption bands were in the same position and the intensity of the bands was minimally altered. This indicated that limited structural alteration occurred. This is consistent with little changes in XRD patterns and quantitative analysis of kaolinite after an acid or alkali spill (Fig. 1 and Table S1). It is also supported by the results of the titration experiment in which surface reaction constants and site density did not appreciably change as a result of an acid or alkali spill (Table 2). In addition, previous studies revealed the similar result that kaolinite, which is one of the non-swelling minerals, is the most resistant clay mineral to acid or alkali attacks^{8,34}.

The acid- or alkali-spilled montmorillonite showed different FT-IR spectra compared to those of the untreated montmorillonite (Fig. 3). As a result of acid spill, the intensity of the bands assigned to the isomorphically

substituted octahedral cation sites (i.e., Al-(Mg, Fe, Al)-OH) decreased. This result was probably because of the great amount of dissolution of Fe and Mg in montmorillonite after acid spill (Table 1). It is also supported by the XRD quantitative analysis that the proportion of montmorillonite did not change by acid spills. It implied that the decrease in the basal site density of the acid-spilled montmorillonite was due to the dissolution of isomorphically substituted octahedral cation sites. In addition, acid spill decreased the intensity of the band for the Si-O-Si sites of montmorillonite, while the Si-O band at 1080 cm^{-1} was shifted to 1090 cm^{-1} at which the Si-O band of cristobalite was assigned³¹. Together with the results of the XRD quantitative analysis (Table S1), the FT-IR spectra indicated that acid spills dissolved Si from montmorillonite and cristobalite was formed. Madejová also observed the similar trend in smectite that the amorphous silica was newly formed after acid treatment³².

In contrast to acid spill, alkali spill increased the intensity of the band assigned to the isomorphically substituted octahedral cation sites of montmorillonite, which corresponds with the optimized basal site density in Table 2. Alkali spill increased basal site density by about 10% (Table 2), which matched with the increasing ratio of montmorillonite by alkali spills (Table S1); Thus, the possible reason for the increase can be ascribed to the enrichment of montmorillonite by alkali spill. Regarding the Si environment in montmorillonite, alkali spill decreased the intensity of Si-O bands of quartz and cristobalite at 778 , and 798 cm^{-1} , respectively, which is consistent with the XRD results of alkali-spilled montmorillonite. The absorption band assigned to the Si-O of the tetrahedral sheet, which was not observed in the untreated or acid-spilled montmorillonite, appeared in the alkali-spilled montmorillonite at 1041 cm^{-1} . In addition, the intensity of the band assigned to hydroxyl group at 3627 cm^{-1} increased by alkali spills, which corresponds to the increase in the edge site density of alkali-spilled montmorillonite from titration experiment (Table 2). According to Table 2, the alkali-spilled montmorillonite had different K_a values with those of the untreated montmorillonite. The results of FT-IR analysis and optimized K_a values indicate that alkali spills increased the proportion of montmorillonite by dissolving quartz and cristobalite, and also changed the surface functional groups' properties by forming new AlOH and SiOH in montmorillonite.

FT-IR spectra demonstrated that montmorillonite was more vulnerable to acid or alkali spills compared to kaolinite, and had good agreement with the optimized site density (Table 2). This was probably because H^+ and OH^- could attack not only the edges but also the swollen interlayer of the montmorillonite^{8,34}. The results indicated that the extent of change in the surface properties resulting from an acid or alkali spill varied with the type of clay mineral, and especially, an expandability should be carefully considered.

Interpretation of the change in K_{a2} using first principle molecular dynamics results. Experimentally derived K_a represented the average K_a of the reactive edge sites in the clay minerals. It is difficult to directly compare the K_a derived from the titration experiment to those calculated from first principle molecular dynamics (FPMD)^{35,36}. In addition, the interpretation of $\text{p}K_{a1}$, generally less than 0, optimized from the titration experiment was inherently limited because the titration data at the pH near $\text{p}K_{a1}$ were meaningless because of the dissolution of the clay minerals. However, a previous study showed that the experimental K_{a2} , optimized by assuming one edge site with a constant capacitance model, well matched the K_a calculated from FPMD³⁷; thus, it is possible to interpret $\text{p}K_{a2}$ in terms of the theoretically calculated $\text{p}K_a$. Liu *et al.* compared the optimized K_a values of kaolinite and montmorillonite from various titration experiments with the theoretical values calculated based on FPMD; these values are summarized in Supplementary Table S2^{37,38}. The $\text{p}K_a$ values of three different kaolinite and montmorillonite samples optimized from this study coincided well with the calculated and experimentally fitted values from other references. This indicated that the edge sites detected from the titration experiments represented surface functional groups as summarized in Supplementary Table S2.

The $\text{p}K_{a2}$ of the untreated and acid-spilled kaolinite (5.49 and 5.94) was similar to calculated $\text{p}K_a$ of AlOH sites of kaolinite (5.7), while that of the alkali-spilled kaolinite (6.34) was near the average value of calculated $\text{p}K_a$ of AlOH and SiOH sites of kaolinite (6.3). However, considering little changes in kaolinite samples' titration curves, XRD, and FT-IR, the differences in $\text{p}K_a$ values were just theoretically generated during the optimization process. In case of montmorillonite, the $\text{p}K_{a2}$ of the untreated montmorillonite (7.32) was similar with the average value of calculated $\text{p}K_a$ of SiOH and AlOH sites of montmorillonite (7.87), while that of the acid-spilled montmorillonite (5.42) was near the calculated $\text{p}K_a$ of AlOH sites of montmorillonite (approximately 5.5). It indicated that acid spills decreased SiOH sites of montmorillonite and this is consistent with FT-IR spectra results that acid spills dissolved Si from the untreated montmorillonite and formed the cristobalite. Because theoretical $\text{p}K_a$ of edge sites was calculated from pure clay minerals, the formation of cristobalite would make $\text{p}K_a$ of the acid-spilled montmorillonite further different from the untreated montmorillonite. Also, decrease in substituted octahedral sites of the acid-spilled montmorillonite might affect $\text{p}K_{a2}$, because isomorphous substitutions increased the adjacent edge sites' $\text{p}K_a$ ^{37,38}. In the case of the alkali-spilled montmorillonite, $\text{p}K_{a2}$ (6.78) was between that of the untreated and acid-spilled montmorillonite. Both SiOH and AlOH increased after alkali spills (Fig. 3); thus $\text{p}K_{a2}$ changed less than the acid-spilled montmorillonite. These results indicated that changes in $\text{p}K_{a2}$ by acid or alkali spills was primarily because of dissolution or formation of surface functional groups, which have different theoretical $\text{p}K_a$ values.

Effect of acid or alkali spills on pH buffering capacity. The pH buffering capacity was the reciprocal of the slope of the titration curve, and it was calculated from the following Equation (1):

$$\text{pH buffering capacity at pH}x = - \left(\text{TOT}H_{\text{pH}x+0.1} - \text{TOT}H_{\text{pH}x} \right) / 0.1 \quad (1)$$

where, $\text{TOT}H_{\text{pH}x}$ (mol L^{-1}) is the total amount of proton added to the suspension of clay minerals during the titration until the suspension pH reaches a value of x . Because the initial pH of the suspension of all the clay minerals ranged from 5.5 to 6.5, the pH buffering capacity at pH 5.5, 6.0 and 6.5 was calculated from the titration curves predicted by using surface complexation modeling under 0.001 M NaNO_3 condition (Fig. 4).

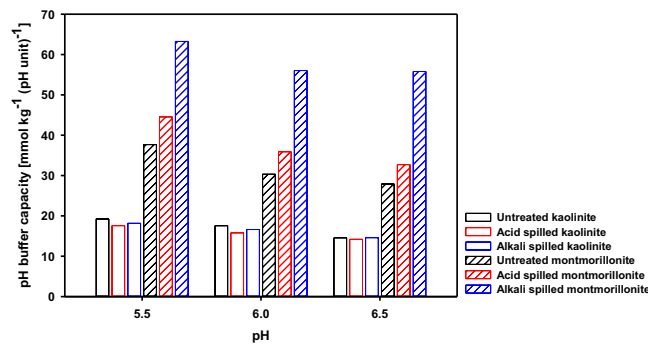


Figure 4. pH buffering capacity of three different kaolinite and montmorillonite samples at pH 5.5, 6.0, and 6.5. Open and cross-hatched bars represent kaolinite and montmorillonite, respectively, and black, red, and blue bars represent untreated, acid-spilled, and alkali-spilled kaolinite or montmorillonite, respectively.

Acid or alkali spills slightly decreased the pH buffering capacity of the kaolinite at pH 5.5, 6.0, and 6.5 from 19.2, 17.6, and 14.6 mmol kg⁻¹ to 17.6 or 18.2, 15.8 or 16.6, and 14.2 or 14.6 mmol kg⁻¹, respectively. In the case of montmorillonite, these spills increased the pH buffering capacity at pH 5.5, 6.0 and 6.5 from 37.7, 30.3 and 27.9 mmol kg⁻¹ to 44.5 or 63.2, 35.9 or 56.0, and 32.7 or 55.8 mmol kg⁻¹, respectively. Because the surface reaction constants and site density determined the pH buffering capacity, the pH buffering capacity of montmorillonite, of which the surface properties were greatly altered by the acid or alkali spills compared to those of kaolinite, was more affected by these spills than kaolinite.

Acid or alkali spills do not result in meaningful changes in the pH buffering capacity of kaolinite, but, unexpectedly, increased the pH buffering capacity of montmorillonite. It indicated that acid or alkali spills do not have an adverse effect on the pH buffering capacity of clay minerals, which is the indicator of soil functions, after neutralization. However, in reality, soils contain not only clay minerals, but also organic matter; thus, the pH buffering capacity of acid- or alkali-spilled soils could change in a different manner from that of a single clay mineral alone. Organic matter is known as the most important component determining pH buffering²³, and it may have a pH buffering capacity 300 times higher than that of kaolinite³⁹. Because acid or alkali spills would decrease organic matter contents via desorption and dissolution^{14–16}, these spills might cause a decrease in the pH buffering capacity of acid- or alkali-spilled soils despite an increase in the pH buffering capacity of single clay minerals. Nevertheless, the results of the pH buffering capacity of clay minerals in this study clearly show that the pH buffering capacity was not deteriorated, but rather increased in montmorillonite after acid or alkali spills.

Conclusions

In this study, we investigated the change in surface properties of clay minerals due to acid or alkali spills and its effect on the pH buffering capacity as an indicator of soil functions. Surface complexation modeling indicated that acid or alkali spills did not significantly change the site density of surface functional groups and their surface acidity constants in kaolinite. In contrast, acid or alkali spills greatly changed the site density and surface acidity constants of montmorillonite. Acid spills dissolved isomorphically substituted octahedral cations and SiOH sites in montmorillonite. In addition, alkali spills dissolved the quartz and cristobalite and edge sites such as AlOH and SiOH sites were newly formed in montmorillonite. Regarding the pH buffering capacity of clay minerals, acid or alkali spills did not have an adverse effect on it, but rather increased in montmorillonite. Soil generally contains organic matter, which plays a significant role in pH buffering, and thus further research with field soil is needed to delineate the effect of acid or alkali spills.

Materials and Methods

Preparation and characterization of clay minerals. KGa-1b kaolinite (Georgia) and SWy-3 montmorillonite (Wyoming) were purchased from the Clay Minerals Society's Source Clays Repository. All chemicals used in this study were of extra pure or reagent grade. The clay minerals were prepared following a similar procedure to the best practices for analyzing surface properties of montmorillonite reviewed by Duc *et al.*^{40–43}. Thirty grams of kaolinite and montmorillonite was dispersed in 1 L of deionized water with a specific resistance of 18.2 M Ω m (Milipore, Bedford, Ma, USA) for 4 h. Prior to the size separation, the pH value of the kaolinite suspension was adjusted to 9.5 by adding NaOH (98%, Daejung, Korea) to facilitate a dispersion. The <2- μ m fraction of each clay mineral was collected via centrifugation (119 g, 5 min). This fraction was washed with 1 M NaNO₃ (99%, Daejung, Korea) and HNO₃ (60%, Daejung, Korea) solution at pH 3 and the supernatant was decanted after centrifugation. This decarbonating procedure was repeated until the supernatant pH reached 3^{41,42,44–46}. The clay minerals were then collected via centrifugation and washed three times with 1 M NaNO₃ solution to change the clays to a Na⁺ form. Although three washing cycles with NaNO₃ might not be enough to make clay minerals homoionic⁴⁷, this pretreatment was chosen to allow for closer comparisons to previous studies, which determined clay minerals' Ka and site density through surface complexation modeling^{30,44,48}. Excess Na⁺ was removed by washing five times with deionized water, and the final pH was in the range from 6 to 7. The collected clay minerals were freeze-dried, and the clay minerals are referred to as untreated clay minerals.

The CEC of untreated kaolinite and montmorillonite, measured ammonium ion through the ammonium acetate method⁴⁹, was 44 and 832 mmol kg⁻¹, respectively. The specific surface areas of the untreated kaolinite and

montmorillonite, obtained using N₂-Brunauer–Emmett–Teller (BET) analysis (ASAP2020, Micromeritics, USA) through adsorption (32 points) and desorption (23 points) isotherms (see in Supplementary Fig. S4)⁵⁰, were 12.10 and 33.75 m² g⁻¹, respectively. These values were used as parameters for the surface complexation modeling^{30,51–54}.

Acid or alkali spill and neutralization. HCl (35%, Daejung, Korea) and NaOH were selected as the strong acid and alkali, respectively, based on their frequency of chemical accidents and amount of use^{1,3}. One gram of the untreated kaolinite or montmorillonite was placed in a 50-mL conical tube and 45 mL of 5 M HCl or NaOH was added to simulate an extreme acid or alkali spill situation. Whole reactions were conducted in a rotating shaker at 25 °C and 40 rpm for two days. The suspension was centrifuged and the supernatant solutions were filtered through a 0.22- μ m filter (Whatman, UK). After acid or alkali spill experiments, the treated solutions were analyzed by using inductively coupled plasma optical emission spectrometry (ICP-OES, iCAP 7400, Thermo Fisher Scientific, USA) to determine the dissolution of the major structural constituents of kaolinite and montmorillonite such as Al, Si, Fe, and Mg.

Separated kaolinite or montmorillonite were washed with deionized water five times to remove excess salts and dissolved ions. A neutralization process was needed because excess H⁺ and OH⁻ remaining after washing and decanting could affect the titration experiment. Thus, the washed kaolinite or montmorillonite were neutralized by adding HNO₃ or NaOH until the supernatant pH reached a neutral pH range. The suspensions were centrifuged and decanted and then residual clay minerals were washed three times with 1 M NaNO₃ to make them homoionic. These clay minerals were washed five times with deionized water, and then freeze-dried. The concentrations of Al and Si in the suspensions were measured by ICP-OES to check the remaining ions' concentration, and they were below one mg kg⁻¹. The whole experiments of acid or alkali spills and neutralization were carried out in triplicates. The XRD analysis was conducted to analyze the mineral identity of the acid- or alkali-spilled clay minerals. The CEC of acid- or alkali-spilled kaolinite was 4.7 cmol kg⁻¹, while that of acid- or alkali-spilled montmorillonite was 737 and 925 mmol kg⁻¹, respectively. The specific surface area of the acid- or alkali-spilled kaolinite was 13.60 and 14.14 m² g⁻¹, respectively, while that of the acid- or alkali-spilled montmorillonite was 34.88 and 19.32 m² g⁻¹, respectively (see in Supplementary Fig. S4).

Potentiometric titration. Potentiometric titration has been used to quantify the density of active reaction sites of clay minerals and determine the surface acidity constants (K_a) of those sites^{25,26,43,44,46,54–61}. The protonation behaviors of three different kaolinite or montmorillonite (untreated, acid-spilled, and alkali-spilled) were investigated using an automatic potentiometric titrator (G10S, Mettler-Toledo, Switzerland). Duc *et al.* recommended the best experimental conditions for the titrations to analyze the acid-base properties of montmorillonite^{42,43,62}, and we adapted the procedure with some modifications as follows.

All titration experiments were performed within a pH range of 4–9 at 25 ± 1 °C under an N₂-purging condition. Deionized water was boiled to remove CO₂ before making clay suspensions and the base titrant. Kaolinite (0.1 g) or montmorillonite (0.05 g) was dispersed in 50 mL of background electrolyte (NaNO₃) solution, and the suspensions were purged with N₂ for 1 h to exclude CO₂. The suspensions were continuously stirred and purged with N₂ during each titration. Titrations of each clay suspension were conducted at three different concentrations of NaNO₃ (0.1, 0.01, and 0.001 M) to investigate the effect of the background electrolytic concentration. Titrant solutions (0.1 M HNO₃ or NaOH), also purged with N₂, were added to the suspensions as 5–10- μ L increments every 5 min, and the pH was automatically recorded. Previous research has demonstrated that a short time interval between successive increments of titrant, generally less than 10 min, is reasonable to minimize mineral dissolution^{43,46,56,59,63}. Drifts in the measured potential were less than 1 mV min⁻¹ in all titration experiments. Two independent titrations of each clay suspension, from initial pH to pH 4 and from initial pH to pH 9, were conducted and combined to obtain one titration curve ranging from pH 4 to 9. This pH range was selected because it is known that the dissolution of kaolinite and montmorillonite is negligible in this pH range^{44,57,58}. In addition, to check the reversibility of titration experiments, titrations from pH 4 to pH 9 were conducted at 0.01 M NaNO₃ condition.

X-ray diffraction measurement. X-ray diffraction (XRD) pattern of the samples of kaolinite and montmorillonite was measured with a X-ray diffractometer (D8 ADVANCE with DAVINCI, Bruker, German) using Cu K α radiation with a λ of 1.5418 Å and a Lynxeye-XE detector operating at 40 kV and 40 mA at a scan rate of 2.4° min⁻¹ from 5° to 80°. The TOPAS Rietveld analysis of XRD patterns was used to quantify the content of mineral components of kaolinite samples. Since it is not precise and difficult to quantify montmorillonite by Rietveld analysis due to the stacking disorder^{64,65}, the fraction of constituents was analyzed semi-quantitatively by comparing the integrated intensities of the diffraction peaks of each constituents⁶⁶.

Fourier-transform infrared spectroscopy. Fourier-transform infrared (FT-IR) spectroscopy was used to investigate the mineralogical and chemical structure and active surface sites of clay minerals for surface acidity^{31,32}. Clay samples were dried at 110 °C overnight to minimize water adsorption. KBr pellets were prepared by mixing kaolinite (1.5 mg) or montmorillonite (1 mg) with 240 mg of KBr powder at a pressure of 10 tons. The FT-IR spectra of the pellets with kaolinite or montmorillonite were recorded using an FT-IR spectrometer (Nicolet 6700, Thermo Scientific, USA) with 32 scans at a resolution of 4 cm⁻¹ within the range of 400–4,000 cm⁻¹.

Surface complexation modeling. A constant capacitance model with permanent negatively charged sites on basal plane and variable charged sites on the mineral edges was chosen to model the surface properties of the kaolinite and montmorillonite^{30,37,44}. The former was referred to as basal sites, while the latter as edge sites. A proton exchange reaction occurred on the basal sites of the clay minerals, while a protonation or deprotonation reaction occurred on the edge sites of them. The least square fitting program FITEQL 4.0 was used to optimize the site densities of the kaolinite and montmorillonite and their surface reaction constants from the titration

experiment⁶⁷. The CEC of the kaolinite and montmorillonite was used as the total site density of the kaolinite and the basal site density of the montmorillonite, respectively^{25,30,44}. Surface properties were optimized from titration data at three different concentrations of background electrolyte (0.1, 0.01, and 0.001 M NaNO₃). FITEQL failed to converge without fixing the equilibrium constant of the kaolinite's proton exchange reaction probably because the titration curves of the kaolinite could be well described without considering the basal sites' proton exchange reaction. Thus, pK_H of the kaolinite's proton exchange reaction constant was assumed to be -2.9 (Table 2), which is an averaged value from references^{55,68–70}. Detailed descriptions of the surface complexation modeling used in this study and the optimization process are explained in the Supplementary Information.

Data Availability

The datasets generated during and/or analyzed during the current study are available from the corresponding author on reasonable request.

References

- Kleindorfer, P. R. *et al.* Accident epidemiology and the RMP rule: learning from a decade of accident history data for the US chemical industry. *The Wharton School of the University of Pennsylvania and Office of Emergency Management US Environmental Protection Agency* (2007).
- Chemistry safety clearing-house (CSC) database; <http://csc.me.go.kr> (2018).
- Shin, D. *et al.* The current status of strong acids production, consumption, and spill cases in Korea. *Journal of Soil and Groundwater Environment* **19**, 6–12, <https://doi.org/10.7857/jsge.2014.19.6.006> (2014).
- A study on the method of environmental impact investigation by accident of acidic chemicals; Highlights of NIER-RP2013-235; Ministry of Environment: Seoul, 2013; <http://www.ndsl.kr/ndsl/commons/util/ndslOriginalView.do?dbt=TRKO&cn=TRKO201700008369&rn=&url=&pageCode=PG18> (2013).
- Dai, Z., Liu, Y., Wang, X. & Zhao, D. Changes in pH, CEC and exchangeable acidity of some forest soils in southern china during the last 32-35 years. *Water, Air, and Soil Pollution* **108**, 377–390 (1998).
- Jardine, P., McCarthy, J. & Weber, N. Mechanisms of dissolved organic carbon adsorption on soil. *Soil Science Society of America Journal* **53**, 1378–1385 (1989).
- Kalbitz, K., Solinger, S., Park, J.-H., Michalzik, B. & Matzner, E. Controls on the dynamics of dissolved organic matter in soils: a review. *Soil Science* **165**, 277–304 (2000).
- Jozefaciuk, G. & Bowanko, G. Effect of acid and alkali treatments on surface areas and adsorption energies of selected minerals. *Clays and Clay minerals* **50**, 771–783 (2002).
- Fenn, M. E. *et al.* Status of soil acidification in North America. *Journal of Forest Science* **52**, 3–13 (2006).
- Kastman, K. H., Ghalib, S. & Zagula, S. *In-situ* remediation of a hydrochloric acid spill. In *Proceedings of the Industrial Waste Conference (USA)* (1992).
- Protopopov, N., Seredina, V. & Molokova, L. In *Contaminated Soil 2000: Seventh International FZK/TNO Conference on Contaminated Soil* (Thomas Telford Ltd), 1–671 (2000).
- Goulding, K. W. Soil acidification and the importance of liming agricultural soils with particular reference to the United Kingdom. *Soil Use and Management* **32**, 390–399, <https://doi.org/10.1111/sum.12270> (2016).
- Jiang, J. *et al.* Responses of soil buffering capacity to acid treatment in three typical subtropical forests. *Science of the Total Environment* **563–564**, 1068–1077, <https://doi.org/10.1016/j.scitotenv.2016.04.198> (2016).
- Weng, L., Van Riemsdijk, W. H., Koopal, L. K. & Hiemstra, T. Adsorption of humic substances on goethite: comparison between humic acids and fulvic acids. *Environmental Science and Technology* **40**, 7494–7500 (2006).
- Ulrich, B. & Sumner, M. E. *Soil acidity* (Springer Science & Business Media 2012).
- Chen, H., Koopal, L. K., Xiong, J., Avena, M. & Tan, W. Mechanisms of soil humic acid adsorption onto montmorillonite and kaolinite. *Journal of Colloid and Interface Science* **504**, 457–467, <https://doi.org/10.1016/j.jcis.2017.05.078> (2017).
- Ravichandran, J. & Sivasankar, B. Properties and catalytic activity of acid-modified montmorillonite and vermiculite. *Clays and Clay Minerals* **45**, 854–858 (1997).
- Bhattacharyya, K. G. & Gupta, S. S. Adsorption of a few heavy metals on natural and modified kaolinite and montmorillonite: a review. *Advances in Colloid Interface Science* **140**, 114–131, <https://doi.org/10.1016/j.cis.2007.12.008> (2008).
- Pálková, H., Hronský, V., Jankovič, Lu & Madejová, J. The effect of acid treatment on the structure and surface acidity of tetraalkylammonium-montmorillonites. *Journal of Colloid and Interface Science* **395**, 166–175 (2013).
- Alekseeva, T., Alekseev, A., Xu, R. K., Zhao, A. Z. & Kalinin, P. Effect of soil acidification induced by a tea plantation on chemical and mineralogical properties of Alfisols in eastern China. *Environmental Geochemistry and Health* **33**, 137–148, <https://doi.org/10.1007/s10653-010-9327-5> (2011).
- Nakao, A., Funakawa, S. & Kosaki, T. Hydroxy-Al polymers block the frayed edge sites of illitic minerals in acid soils: studies in southwestern Japan at various weathering stages. *European Journal of Soil Science* **60**, 127–138, <https://doi.org/10.1111/j.1365-2389.2008.01097.x> (2009).
- Van Der Salm, C. & De Vries, W. Soil acidification in loess and clay soils in the Netherlands. *Water, Air, and Soil Pollution* **120**, 139–167 (2000).
- Aitken, R., Moody, P. & McKinley, P. Lime requirement of acidic Queensland soils. I. Relationships between soil properties and pH buffer capacity. *Soil Research* **28**, 695–701 (1990).
- Sposito, G. *The chemistry of soils* (Oxford university press, 2008).
- Bourg, I. C., Sposito, G. & Bourg, A. C. Modeling the acid-base surface chemistry of montmorillonite. *Journal of Colloid and Interface Science* **312**, 297–310, <https://doi.org/10.1016/j.jcis.2007.03.062> (2007).
- Tournassat, C., Davis, J. A., Chiaberge, C., Grangeon, S. & Bourg, I. C. Modeling the acid-base properties of montmorillonite edge surfaces. *Environmental Science and Technology* **50**, 13436–13445, <https://doi.org/10.1021/acs.est.6b04677> (2016).
- Chipera, S. J. & Bish, D. L. Baseline studies of the clay minerals society source clays: powder X-ray diffraction analyses. *Clays and Clay Minerals* **49**, 398–409 (2001).
- Theng, B., Lagaly, G. & Bergaya, F. *Handbook of clay science* (Elsevier, 2006).
- Szekeress, M. & Tombácz, E. Surface charge characterization of metal oxides by potentiometric acid–base titration, revisited theory and experiment. *Colloids and Surfaces A: Physicochemical and Engineering Aspects* **414**, 302–313, <https://doi.org/10.1016/j.colsurfa.2012.08.027> (2012).
- Gu, X. & Evans, L. J. Surface complexation modelling of Cd(II), Cu(II), Ni(II), Pb(II) and Zn(II) adsorption onto kaolinite. *Geochimica et Cosmochimica Acta* **72**, 267–276, <https://doi.org/10.1016/j.gca.2007.09.032> (2008).
- Madejova, J. & Komadel, P. Baseline studies of the clay minerals society source clays: infrared methods. *Clays and Clay Minerals* **49**, 410–432 (2001).
- Madejová, J. FTIR techniques in clay mineral studies. *Vibrational Spectroscopy* **31**, 1–10 (2003).

33. Vicente-Rodríguez, M. A., Suarez, M., Bañares-Muñoz, M. A. & de Dios Lopez-Gonzalez, J. Comparative FT-IR study of the removal of octahedral cations and structural modifications during acid treatment of several silicates. *Spectrochimica Acta Part A: Molecular and Biomolecular Spectroscopy* **52**, 1685–1694 (1996).
34. Jozefaciuk, G. Effect of acid and alkali treatments on surface-charge properties of selected minerals. *Clays and Clay Minerals* **50**, 647–656 (2002).
35. Tazi, S., Rotenberg, B., Salanne, M., Sprik, M. & Sulpizi, M. Absolute acidity of clay edge sites from ab-initio simulations. *Geochimica et Cosmochimica Acta* **94**, 1–11 (2012).
36. Bickmore, B. R., Rosso, K. M., Nagy, K. L., Cygan, R. T. & Tadanier, C. J. Ab initio determination of edge surface structures for dioctahedral 2:1 phyllosilicates: implications for acid-base reactivity. *Clays and Clay Minerals* **51**, 359–371 (2003).
37. Liu, X. *et al.* Acidity of edge surface sites of montmorillonite and kaolinite. *Geochimica et Cosmochimica Acta* **117**, 180–190, <https://doi.org/10.1016/j.gca.2013.04.008> (2013).
38. Liu, X., Cheng, J., Sprik, M., Lu, X. & Wang, R. Surface acidity of 2:1-type dioctahedral clay minerals from first principles molecular dynamics simulations. *Geochimica et Cosmochimica Acta* **140**, 410–417, <https://doi.org/10.1016/j.gca.2014.05.044> (2014).
39. Bache, B. W. Measurements and mechanisms in acid soils. *Communications in Soil Science and Plant Analysis* **19**, 775–792 (1988).
40. Sarkar, D., Essington, M. & Misra, K. Adsorption of mercury (II) by kaolinite. *Soil Science Society of America Journal* **64**, 1968–1975 (2000).
41. Chorover, J. *et al.* Linking cesium and strontium uptake to kaolinite weathering in simulated tank waste leachate. *Environmental Science and Technology* **37**, 2200–2208 (2003).
42. Duc, M., Gaboriaud, F. & Thomas, F. Sensitivity of the acid–base properties of clays to the methods of preparation and measurement. *Journal of Colloid and Interface Science* **289**, 139–147, <https://doi.org/10.1016/j.jcis.2005.03.060> (2005).
43. Duc, M., Gaboriaud, F. & Thomas, F. Sensitivity of the acid–base properties of clays to the methods of preparation and measurement. 2. Evidence from continuous potentiometric titrations. *Journal of Colloid and Interface Science* **289**, 148–156, <https://doi.org/10.1016/j.jcis.2005.03.057> (2005).
44. Gu, X., Evans, L. J. & Barabash, S. J. Modeling the adsorption of Cd (II), Cu (II), Ni (II), Pb (II) and Zn (II) onto montmorillonite. *Geochimica et Cosmochimica Acta* **74**, 5718–5728, <https://doi.org/10.1016/j.gca.2010.07.016> (2010).
45. Guo, Z. *et al.* Eu (III) adsorption/desorption on Na-bentonite: experimental and modeling studies. *Colloids and Surfaces A: Physicochemical and Engineering Aspects* **339**, 126–133 (2009).
46. Wanner, H. *et al.* The acid/base chemistry of montmorillonite. *Radiochimica Acta* **66–67**, <https://doi.org/10.1524/ract.1994.6667.special-issue.157> (1994).
47. Steudel, A. & Emmerich, K. Strategies for the successful preparation of homoionic smectites. *Applied Clay Science* **75–76**, 13–21, <https://doi.org/10.1016/j.clay.2013.03.002> (2013).
48. Chen, M. A. & Kocar, B. D. Radium sorption to iron (hydr)oxides, pyrite, and montmorillonite: implications for mobility. *Environmental Science and Technology* **52**, 4023–4030, <https://doi.org/10.1021/acs.est.7b05443> (2018).
49. Schollenberger, C. & Simon, R. Determination of exchange capacity and exchangeable bases in soil—ammonium acetate method. *Soil Science* **59**, 13–24 (1945).
50. Brunauer, S., Emmett, P. H. & Teller, E. Adsorption of gases in multimolecular layers. *Journal of the American Chemical Society* **60**, 309–319 (1938).
51. Dzombak, D. A. *Surface complexation modeling: hydrous ferric oxide* (John Wiley & Sons, 1990).
52. Kraepiel, A. M., Keller, K. & Morel, F. M. On the acid–base chemistry of permanently charged minerals. *Environmental Science and Technology* **32**, 2829–2838 (1998).
53. Bradbury, M. H. & Baeyens, B. A mechanistic description of Ni and Zn sorption on Na-montmorillonite Part II: modelling. *Journal of Contaminant Hydrology* **27**, 223–248 (1997).
54. Bradbury, M. & Baeyens, B. Sorption of Eu on Na- and Ca-montmorillonites: experimental investigations and modelling with cation exchange and surface complexation. *Geochimica et Cosmochimica Acta* **66**, 2325–2334 (2002).
55. Schindler, P., Liechti, P. & Westall, J. Adsorption of copper, cadmium and lead from aqueous solution to the kaolinite/water interface. *Netherlands Journal of Agricultural Science (Netherlands)* (1987).
56. Brady, P. V., Cygan, R. T. & Nagy, K. L. Molecular controls on kaolinite surface charge. *Journal of Colloid and Interface Science* **183**, 356–364 (1996).
57. Baeyens, B. & Bradbury, M. H. A mechanistic description of Ni and Zn sorption on Na-montmorillonite Part I: Titration and sorption measurements. *Journal of Contaminant Hydrology* **27**, 199–222 (1997).
58. Tournassat, C., Greneche, J. M., Tisserand, D. & Charlet, L. The titration of clay minerals I. Discontinuous backtitration technique combined with CEC measurements. *Journal of Colloid and Interface Science* **273**, 224–233, <https://doi.org/10.1016/j.jcis.2003.11.021> (2004).
59. Tertre, E., Castet, S., Berger, G., Loubet, M. & Giffaut, E. Surface chemistry of kaolinite and Na-montmorillonite in aqueous electrolyte solutions at 25 and 60 °C: Experimental and modeling study. *Geochimica et Cosmochimica Acta* **70**, 4579–4599, <https://doi.org/10.1016/j.gca.2006.07.017> (2006).
60. Komarek, M., Koretsky, C. M., Stephen, K. J., Alessi, D. S. & Chrastny, V. Competitive Adsorption of Cd(II), Cr(VI), and Pb(II) onto nanomaghemite: a spectroscopic and modeling approach. *Environmental Science and Technology* **49**, 12851–12859, <https://doi.org/10.1021/acs.est.5b03063> (2015).
61. Liu, Y. *et al.* Acid-base properties of kaolinite, montmorillonite and illite at marine ionic strength. *Chemical Geology* **483**, 191–200, <https://doi.org/10.1016/j.chemgeo.2018.01.018> (2018).
62. Duc, M., Thomas, F. & Gaboriaud, F. Coupled chemical processes at clay/electrolyte interface: a batch titration study of Na-montmorillonites. *Journal of Colloid and Interface Science* **300**, 616–625, <https://doi.org/10.1016/j.jcis.2006.04.081> (2006).
63. Rozalen, M., Brady, P. V. & Huertas, F. J. Surface chemistry of K-montmorillonite: ionic strength, temperature dependence and dissolution kinetics. *Journal of Colloid and Interface Science* **333**, 474–484, <https://doi.org/10.1016/j.jcis.2009.01.059> (2009).
64. Ufer, K. & Raven, M. D. Application of the Rietveld method in the Reynolds cup contest. *Clays and Clay Minerals* **65**, 286–297 (2017).
65. Lutterotti, L., Voltolini, M., Wenk, H.-R., Bandyopadhyay, K. & Vanorio, T. Texture analysis of a turbostratically disordered Ca-montmorillonite. *American Mineralogist* **95**, 98–103 (2010).
66. Liu, D. *et al.* Quantitative characterization of the solid acidity of montmorillonite using combined FTIR and TPD based on the NH₃ adsorption system. *Applied Clay Science* **80**, 407–412 (2013).
67. Herbelin, A. L. & Westall, J. C. FITEQL: A computer program for determination of chemical equilibrium constants from experimental data. *Version 4*, 99–01 (1999).
68. Angove, M. J., Johnson, B. B. & Wells, J. D. Adsorption of cadmium(II) on kaolinite. *Colloids and Surfaces A: Physicochemical and Engineering Aspects* **126**, 137–147 (1997).
69. Ikhsan, J., Johnson, B. B. & Wells, J. D. A comparative study of the adsorption of transition metals on kaolinite. *Journal of Colloid and Interface Science* **217**, 403–410 (1999).
70. Srivastava, P., Singh, B. & Angove, M. Competitive adsorption behavior of heavy metals on kaolinite. *Journal of Colloid and Interface Science* **290**, 28–38, <https://doi.org/10.1016/j.jcis.2005.04.036> (2005).

Acknowledgements

This work was supported by Korea Environment Industry & Technology Institute through Subsurface Environment Management Project (2018002450002). The authors would like to thank the Institute of Engineering Research at Seoul National University for technical assistance.

Author Contributions

K. Nam directed this research and was the overall in-charge. I. Jeon and K. Nam planned and designed the experiments. I. Jeon performed the experiments and analyzed the data. All authors wrote and reviewed the manuscript.

Additional Information

Supplementary information accompanies this paper at <https://doi.org/10.1038/s41598-019-46175-y>.

Competing Interests: The authors declare no competing interests.

Publisher's note: Springer Nature remains neutral with regard to jurisdictional claims in published maps and institutional affiliations.



Open Access This article is licensed under a Creative Commons Attribution 4.0 International License, which permits use, sharing, adaptation, distribution and reproduction in any medium or format, as long as you give appropriate credit to the original author(s) and the source, provide a link to the Creative Commons license, and indicate if changes were made. The images or other third party material in this article are included in the article's Creative Commons license, unless indicated otherwise in a credit line to the material. If material is not included in the article's Creative Commons license and your intended use is not permitted by statutory regulation or exceeds the permitted use, you will need to obtain permission directly from the copyright holder. To view a copy of this license, visit <http://creativecommons.org/licenses/by/4.0/>.

© The Author(s) 2019